

ASTEROSEISMIC CONSTRAINTS FOR GAIA

O. L. Creevey¹ and F. Thévenin¹

Abstract. Distances from the Gaia mission will no doubt improve our understanding of stellar physics by providing an excellent constraint on the luminosity of the star. However, it is also clear that high precision stellar properties from, for example, asteroseismology, will also provide a needed input constraint in order to calibrate the methods that Gaia will use, e.g. stellar models or `GSP_Phot`. For solar-like stars (F, G, K IV/V), asteroseismic data delivers at the least two very important quantities: (1) the average large frequency separation $\langle \Delta\nu \rangle$ and (2) the frequency corresponding to the maximum of the modulated-amplitude spectrum ν_{\max} . Both of these quantities are related directly to stellar parameters (radius and mass) and in particular their combination (gravity and density). We show how the precision in $\langle \Delta\nu \rangle$, ν_{\max} , and atmospheric parameters T_{eff} and $[\text{Fe}/\text{H}]$ affect the determination of gravity ($\log g$) for a sample of well-known stars. We find that $\log g$ can be determined within less than 0.02 dex accuracy for our sample while considering precisions in the data expected for $V \sim 12$ stars from *Kepler* data. We also derive masses and radii which are accurate to within 1σ of the accepted values. This study validates the subsequent use of all of the available asteroseismic data on solar-like stars from the *Kepler* field (> 500 IV/V stars) in order to provide a very important constraint for Gaia calibration of `GSP_Phot` through the use of $\log g$. We note that while we concentrate on IV/V stars, both the CoRoT and *Kepler* fields contain asteroseismic data on thousands of giant stars which will also provide useful calibration measures.

Keywords: stars:fundamental parameters

1 Introduction

The ESA Gaia¹ mission is due to launch in Autumn 2013. Its primary objective is to perform a 6-D mapping of the Galaxy by observing over 1 billion stars down to a magnitude of $V = 20$. The mission will yield distances to these stars, and for about 20/100 million stars, distances with precisions of less than 1%/10% will be obtained.

Gaia will obtain its astrometry by using broad band “G” photometry (similar to a V magnitude). The spacecraft is also equipped with a spectrophotometer comprising both a blue and a red prism BP/RP, delivering *colour* information. A spectrometer will be used to determine the radial velocities of objects as far as $G = 17$ (precisions from 1–20 kms^{-1}), and for stars with $G < 11$ high resolution spectra ($R \sim 11,500$) will be available.

One of the main workpackages devoted to source characterisation is `GSP_Phot` whose objectives are to obtain stellar properties for 1 billion single stars by using the G band photometry, the parallax π , and the spectrophotometric information BP/RP (Bailer-Jones 2010). The stellar properties that will be derived are effective temperature T_{eff} , extinction A_G in the G band, surface gravity $\log g$, and metallicity $[\text{Fe}/\text{H}]$. Liu et al. (2012) compare different methods to determine these parameters and they estimate typical precisions in $\log g$ on the order of 0.1 - 0.2 dex for main sequence late-type stars, and mean absolute residuals (true value minus inferred value from simulations) no less than 0.1 dex for stars of all magnitudes.

A calibration plan using forty bright benchmark stars has been put in place to deliver the *best* stellar models. These will be used on ~ 5000 calibration stars which will be observed by Gaia. However, for most of these fainter stars $\log g$ remains quite unconstrained, and this will inherently reduce the full capacity of source characterisation with Gaia data.

In the last decade or so, much progress in the field of observational asteroseismology has been made, especially for stars exhibiting Sun-like oscillations. These stars have deep outer convective envelopes where stochastic

¹ Laboratoire Lagrange, CNRS, Université de Nice Sophia-Antipolis, Nice, 06300, France

ⁱ<http://sci.esa.int/science-e/www/area/index.cfm?fareaid=26>

turbulence gives rise to a broad spectrum of excited resonant oscillation modes e.g. Brown & Gilliland 1994. The power spectra of such stars can be characterised by two mean seismic quantities: $\langle\Delta\nu\rangle$ and ν_{\max} . The quantity $\langle\Delta\nu\rangle$ is the mean value of the *large frequency separations* $\Delta\nu_{l,n} = \nu_{l,n} - \nu_{l,n-1}$ where $\nu_{l,n}$ is a frequency with degree l and radial order n , and ν_{\max} is the frequency corresponding to the maximum amplitude of the bell-shaped frequency spectrum. The following scaling relations have also been shown to hold: Eq. 1: $\langle\Delta\nu\rangle \approx M^{0.5}R^{-1.5}\langle\Delta\nu\rangle_{\odot}$ and Eq. 2: $\nu_{\max} \approx MR^{-2}(T_{\text{eff}}/5777)^{-0.5}\nu_{\max,\odot}$ (Eq. 1) where $\langle\Delta\nu\rangle_{\odot} = 134.9 \mu\text{Hz}$ and $\nu_{\max,\odot} = 3,050 \mu\text{Hz}$ (Kjeldsen & Bedding 1995).

Of particular interest for Gaia is the *Kepler* (<http://kepler.nasa.gov>) field of view — ~ 100 square-degrees, centered on galactic coordinates $76.32^{\circ}, +13.5^{\circ}$. *Kepler* is a NASA mission dedicated to characterising planet-habitability (Borucki et al. 2010). It obtains photometric data of $\sim 150,000$ stars with a typical cadence of 30 minutes. A subset of stars (< 1000 every month) acquire data with a point every 1 minute. This is sufficient to detect and characterise Sun-like oscillations in many stars. Verner et al. (2011) and Chaplin et al. (2011) recently showed the detections of these mean seismic quantities for a sample of >500 F, G, K IV/V stars with typical magnitudes $7 < V < 12$, while both CoRoT and *Kepler* have both shown their capabilities of detecting these same seismic quantities in 1000s of red giants (Hekker et al. 2009; Baudin et al. 2011; Mosser et al. 2012).

With the detection of mean seismic quantities in hundreds of stars, the *Kepler* field is very promising for helping to calibrate the `GSP_Phot` methods. In particular, they deliver one of the four stellar properties to be extracted by automatic analyses of Gaia data, namely $\log g$. Gai et al. (2011) studied the distribution of errors for a sample of simulated stars using seismic data and a grid-based method based on stellar evolution models. They concluded that a seismic $\log g$ is almost fully independent of the input physics in the stellar evolution models that are used. More recently Morel & Miglio (2012) compared classical determinations of $\log g$ to those derived alone from the scaling relation (Eq. [2]), and concluded that the mean differences between the various methods used is ~ 0.05 dex, thus supporting the validity of a seismic determination of $\log g$. However, to date, no study has been done to validate the *accuracy* of a seismic $\log g$ (how closely it resembles the true value) by using stars with measured radii and masses. This is the objective of this work.

2 A comparison of the direct and seismic methods for determining $\log g$.

2.1 Observations and direct determination of $\log g$

We aim to compare an *asteroseismically* derived $\log g$ with the true known value for a sample of stars. We chose a sample of seven bright well-characterised stars for which the radius is known via interferometry or a binary solution and the mass is known from either the binary solution or a detailed seismic analysis. Table 1 lists the sample of stars along with the observed values of $\langle\Delta\nu\rangle$, ν_{\max} , T_{eff} , $[\text{Fe}/\text{H}]$, M , and R . The final column in the table gives the *true* value of $\log g$ derived from M and R .

2.2 Seismic method to determine $\log g$

We use a grid-based method, RadEx10, to determine an asteroseismic value of $\log g$ (Creevey et al. 2012). The grid was constructed using the ASTEC stellar evolution code (Christensen-Dalsgaard 2008) without diffusion effects and the same input physics as described in Creevey et al. (2012).

The grid considers models with masses M from $0.75 - 2.0 M_{\odot}$ in steps of $0.05 M_{\odot}$, ages t from ZAMS to subgiant, the initial chemical composition Z_i (metallicity) spans $0.007 - 0.027$ in steps of ~ 0.003 , while X_i (hydrogen) is set to 0.70: this corresponds to an initial He abundance $Y_i = 0.263 - 0.283$. The mixing length parameter $\alpha = 2.0$ is used, which was obtained by calibrating it with solar data.

To obtain the grid-based model stellar properties ($\log g$, M , R , L , t) we perturb the set of input observations using a random Gaussian distribution, and compare the perturbed observations to the model ones. The input observations consist primarily of $\langle\Delta\nu\rangle$, ν_{\max} , T_{eff} , and $[\text{Fe}/\text{H}]$, although other inputs are possible, for example, L or R . The stellar parameters and uncertainties are defined as the mean value of the fitted parameter from 10,000 realizations, with the standard deviations defining the 1σ uncertainties.

2.3 Analysis approach

We determine a seismic $\log g$ for the stars using the method explained above, and the following data sets:

(S1) $\{\langle\Delta\nu\rangle, \nu_{\max}, T_{\text{eff}}, [\text{Fe}/\text{H}]\}$,

Table 1. Observed properties of the reference stars

Star	$\langle\Delta\nu\rangle$ (μHz)	ν_{max} (mHz)	T_{eff} (K)	[Fe/H] (dex)	R (R_{\odot})	M (M_{\odot})	$\log g$ (dex)
αCenB	161.5 ± 0.11^{1a}	4.0^{1a}	5316 ± 28^{1b}	0.25 ± 0.04^{1b}	0.863 ± 0.005^{1c}	0.934 ± 0.0061^{1d}	4.538 ± 0.008
18 Sco	134.4 ± 0.3^{2a}	3.1^{2a}	5813 ± 21^{2a}	0.04 ± 0.01^{2a}	1.010 ± 0.009^{2a}	1.02 ± 0.03^{2a}	4.438 ± 0.005
Sun	134.9 ± 0.1^{3a}	3.05^{3b}	5778 ± 20^{3c}	0.00 ± 0.01^{3d}	1.000 ± 1.010^{3d}	1.000 ± 0.010^{3d}	4.438 ± 0.002
αCenA	105.6^{4a}	2.3^{4a}	5847 ± 27^{1b}	0.24 ± 0.03^{1b}	1.224 ± 0.003^{1c}	1.105 ± 0.007^{1d}	4.307 ± 0.005
HD 49933	85.66 ± 0.18^{5a}	1.8^{5a}	6500 ± 75^{5b}	-0.35 ± 0.10^{5b}	1.42 ± 0.04^{5c}	1.20 ± 0.08^{5c}	4.212 ± 0.039
Procyon	55.5 ± 0.5^{6a}	1.0^{6b}	6530 ± 90^{6c}	-0.05 ± 0.03^{6d}	2.067 ± 0.028^{6e}	1.497 ± 0.037^{6f}	3.982 ± 0.016
βHydri	57.24 ± 0.16^{7a}	1.0^{7a}	5872 ± 44^{7b}	-0.10 ± 0.07^{7c}	1.814 ± 0.017^{7b}	1.07 ± 0.03^{7b}	3.950 ± 0.015

References: ^{1a}Kjeldsen et al. (2005), ^{1b}Porto de Mello et al. (2008), ^{1c}Kervella et al. (2003), ^{1d}Pourbaix et al. (2002), ^{2a}Bazot et al. (2011), ^{3a}Taking the average of Table 3 from Toutain & Froehlich (1992), ^{3b}Kjeldsen & Bedding (1995), ^{3c}Grevesse & Sauval (1998), ^{3d}We adopt a typical error of 0.01 in [Fe/H], M and R , ^{4a}Bouchy & Carrier (2002), ^{5a}Using the $l = 0$ modes with Height/Noise > 1 from Table 1 of Benomar et al. (2009), ^{5b}Kallinger et al. (2010) $Z = 0.008\pm 0.002$ is referenced, ^{5c}Bigot et al. (2011), ^{6a}Eggenberger et al. (2004), ^{6b}Martić et al. (2004), ^{6c}Fuhrmann et al. (1997), ^{6d}Allende Prieto et al. (2002), ^{6e}Kervella et al. (2004), ^{6f}Girard et al. (2000), ^{7a}Bedding et al. (2007), ^{7b}North et al. (2007), ^{7c}Bruntt et al. (2010).

(S2) $\{\langle\Delta\nu\rangle, \nu_{\text{max}}, T_{\text{eff}}\}$, and

(S3) $\{\langle\Delta\nu\rangle, \nu_{\text{max}}\}$.

For the potential sample of Gaia calibration stars, [Fe/H] is not always available, and in some cases, a photometric T_{eff} may have various estimations. For these reasons we include S2 and S3.

The observational errors in our sample are very small due to the brightness and proximity of the star, so we also derive an asteroseismic $\log g$ while considering observational errors that we expect for *Kepler* stars (see Verner et al. 2011). We consider three types of observational errors:

(E1) the true measurement errors from the literature,

(E2) typically “good” errors, i.e. $\sigma(\langle\Delta\nu\rangle, \nu_{\text{max}}, T_{\text{eff}}, [\text{Fe}/\text{H}]) = 0.5 \mu\text{Hz}, 5\%, 70 \text{ K}, 0.08 \text{ dex}$,

(E3) “not-so-good” errors (e.g. $V \sim 11, 12$), $\sigma(\langle\Delta\nu\rangle, \nu_{\text{max}}, T_{\text{eff}}, [\text{Fe}/\text{H}]) = 1.1 \mu\text{Hz}, 8\%, 110 \text{ K}, 0.12 \text{ dex}$.

2.4 Seismic versus direct $\log g$

In Figure 1 we compare the asteroseismic $\log g$ with the true $\log g$ for the seven stars. Each star is represented by a point on the abscissa, and the y-axis shows (seismic - true) value of $\log g$. There are three panels which represent the results using the three different subsets of input data. We also show for each star in each panel three results; in the bottom left corner these are marked by ‘E1’, ‘E2’, and ‘E3’, and represent the results using the different errors in the observations. The black dotted lines represent (seismic - true) $\log g = 0$, and the grey dotted lines indicate $\pm 0.01 \text{ dex}$.

Figure 1 shows that for all observational sets and errors $\log g$ is generally estimated to within 0.02 dex in both precision and accuracy. This result clearly shows the validity of the mean seismic quantities and atmospheric parameters for providing an extremely precise value of $\log g$. Other general trends that can be seen are that the typical *precision* in $\log g$ decreases as (1) the observational errors increase (from E1 – E3), and (2) the information content decreases (S1 – S2 – S3, for example). One noticeable result is the systematic offset in the derivation of $\log g$ for HD 49933 when we use [Fe/H] as input (S1). This could be due to an incorrect metallicity, an error in the adopted true $\log g$ or a shortcoming of the grid of models.

Figure 2 shows the *seismic* radius and mass determinations of the sample stars using S1 while considering the three sets of errors. We find that with *good* observational errors, the radii are matched to within 1% (accuracy) with typical precisions of 2–3%, while the masses are matched to within 1–4% with typical precisions of 4–7%. Here it can be seen that the offset found for HD 49933 in $\log g$ is related to the reference mass value (the radius seems to be consistent). For S2 and S3 the uncertainties begin to grow very large; 2–5% and 3–10%, respectively in radius, and 5–15% and 10–35% in mass, while the accuracies also decrease (not shown) although to within $< 1.5\sigma$ for all results. These results indicate that for the most precise determination of mass and radius, a seismic index and both T_{eff} and [Fe/H] are necessary, unlike $\log g$ where the seismic information alone

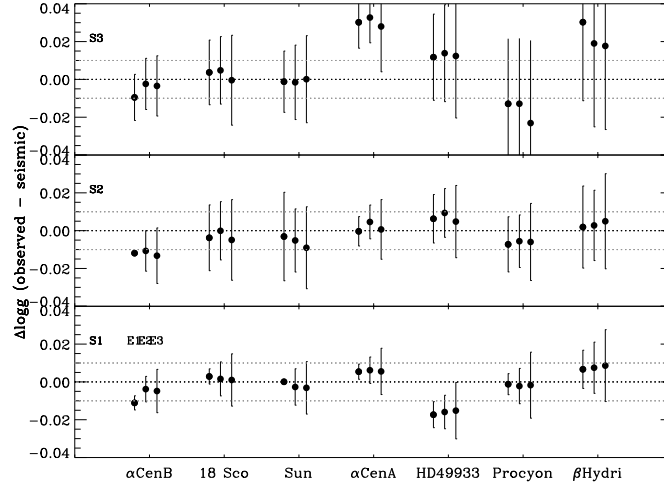


Fig. 1. *Seismic-minus-true* $\log g$ for the seven sample stars while considering different sets of input observations (different panels) and different observational errors (E1, E2, E3).

Table 2. Stellar properties for the reference stars derived by RadEx10

Star	$\log g(\text{dex})$	$R (R_{\odot})$	$M (M_{\odot})$	$L (L_{\odot})$	Age (Gyr)
α Cen B	4.527 ± 0.004	0.859 ± 0.007	0.905 ± 0.023	0.52 ± 0.02	9.4 ± 2.0
18 Sco	4.441 ± 0.004	1.018 ± 0.008	1.042 ± 0.019	1.07 ± 0.04	4.8 ± 0.9
Sun	4.438 ± 0.001	1.000 ± 0.002	1.000 ± 0.005	1.01 ± 0.03	6.3 ± 0.6
α Cen A	4.312 ± 0.004	1.223 ± 0.010	1.119 ± 0.024	1.56 ± 0.08	7.0 ± 0.9
HD 49933	4.195 ± 0.007	1.418 ± 0.022	1.148 ± 0.054	3.23 ± 0.22	3.5 ± 0.6
Procyon	3.981 ± 0.006	2.072 ± 0.024	1.497 ± 0.041	7.08 ± 0.54	2.1 ± 0.2
β Hydri	3.957 ± 0.010	1.840 ± 0.045	1.119 ± 0.086	3.55 ± 0.31	6.8 ± 1.0

(or including T_{eff}) can produce an accurate result.

2.5 Systematic errors in observations

To study the effect of *systematic errors* in the atmospheric parameters, we repeated our analysis for β Hydri using three sets of input data that change only in T_{eff} and $[\text{Fe}/\text{H}]$ considering the E2 errors. The first set (1) uses the North et al. (2007) values (5872, -0.10), the second set (2) uses (5964, -0.10), and the third set (3) uses da Silva et al. (2006) values (5964, -0.03). For S1 we derived $\log g = 3.96, 3.97,$ and 3.97 dex for case 1, 2, and 3, respectively (ref. value is 3.95 dex). Excluding $[\text{Fe}/\text{H}]$ (S2) we derived $\log g = 3.95$ and 3.96 for case 1 and 2, respectively. Here we can conclude that errors in the atmospheric parameters can change $\log g$ by up to 0.02 dex, and in the absence of an accurate $[\text{Fe}/\text{H}]$ it is better to exclude it. To determine the mass, radius,

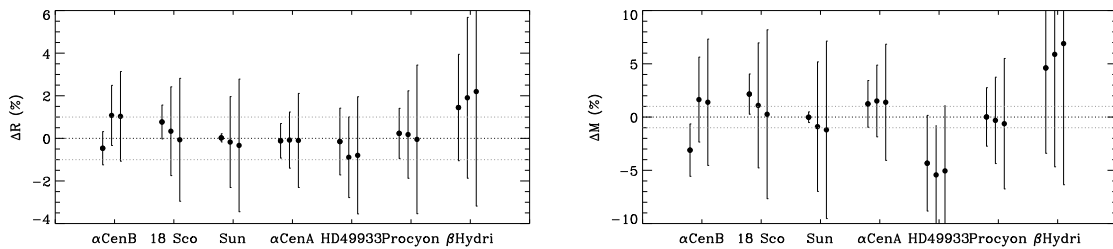


Fig. 2. *Seismic-minus-True* values of radius (left panel) and mass (right panel) using S1.

and age, however, $[\text{Fe}/\text{H}]$ is a very important constraint.

3 Conclusions

We summarize the stellar properties of the sample stars in Table 2 derived by RadEx10 using $\langle\Delta\nu\rangle$, ν_{max} , T_{eff} , and $[\text{Fe}/\text{H}]$, and the true observational errors. We highlight the excellent agreement between seismically determined parameters and those obtained by direct mass and radius estimates (compare Tables 1 and 2). In only two cases (α Cen B and 18 Sco), we find that $\log g$ and mass are determined with a difference of just over 1σ for S1 and S3, while for S2 we find that $\log g$ is accurate to within its σ for all stars. This study validates the accuracy of a seismically determined $\log g$ while also highlighting the excellent precision that can be obtained using seismic data. If we relax the observational errors to those typical of what is available for the sample of ~ 500 *Kepler* F, G, K IV/V *Kepler* stars, then we obtain $\log g$ with precisions of less than 0.02 dex for S1 (including $[\text{Fe}/\text{H}]$ as a measurement) and less than 0.03 dex for S2 (excluding $[\text{Fe}/\text{H}]$) for even “poor” observational errors on the input seismic and atmospheric data. We also showed that we can expect to find a typical systematic error of no bigger than 0.02 dex arising from an error in the atmospheric parameters.

OLC is a Henri Poincaré Fellow at OCA, funded by the Conseil Général des Alpes-Maritimes and OCA.

References

- Allende Prieto, C., Asplund, M., García López, R. J., & Lambert, D. L. 2002, *ApJ*, 567, 544
 Bailer-Jones, C. A. L. 2010, *MNRAS*, 403, 96
 Baudin, F., Barban, C., Belkacem, K., et al. 2011, *A&A*, 529, A84
 Bazot, M., Ireland, M. J., Huber, D., et al. 2011, *A&A*, 526, L4
 Bedding, T. R., Kjeldsen, H., Arentoft, T., et al. 2007, *ApJ*, 663, 1315
 Benomar, O., Baudin, F., Campante, T. L., et al. 2009, *A&A*, 507, L13
 Bigot, L., Mourard, D., Berio, P., et al. 2011, *A&A*, 534, L3
 Borucki, W. J., Koch, D., Basri, G., et al. 2010, *Science*, 327, 977
 Bouchy, F. & Carrier, F. 2002, *A&A*, 390, 205
 Brown, T. M. & Gilliland, R. L. 1994, *ARAA*, 32, 37
 Bruntt, H., Bedding, T. R., Quirion, P.-O., et al. 2010, *MNRAS*, 405, 1907
 Chaplin, W. J., Kjeldsen, H., Christensen-Dalsgaard, J., et al. 2011, *Science*, 332, 213
 Christensen-Dalsgaard, J. 2008, *Ap&SS*, 316, 13
 Creevey, O. L., Doğan, G., Frasca, A., et al. 2012, *A&A*, 537, A111
 da Silva, L., Girardi, L., Pasquini, L., et al. 2006, *A&A*, 458, 609
 Eggenberger, P., Carrier, F., Bouchy, F., & Blecha, A. 2004, *A&A*, 422, 247
 Fuhrmann, K., Pfeiffer, M., Frank, C., Reetz, J., & Gehren, T. 1997, *A&A*, 323, 909
 Gai, N., Basu, S., Chaplin, W. J., & Elsworth, Y. 2011, *ApJ*, 730, 63
 Girard, T. M., Wu, H., Lee, J. T., et al. 2000, *AJ*, 119, 2428
 Grevesse, N. & Sauval, A. J. 1998, *Space Sci. Rev.*, 85, 161
 Hekker, S., Kallinger, T., Baudin, F., et al. 2009, *A&A*, 506, 465
 Kallinger, T., Gruberbauer, M., Guenther, D. B., Fossati, L., & Weiss, W. W. 2010, *A&A*, 510, A106
 Kervella, P., Thévenin, F., Morel, P., et al. 2004, *A&A*, 413, 251
 Kervella, P., Thévenin, F., Ségransan, D., et al. 2003, *A&A*, 404, 1087
 Kjeldsen, H. & Bedding, T. R. 1995, *A&A*, 293, 87
 Kjeldsen, H., Bedding, T. R., Butler, R. P., et al. 2005, *ApJ*, 635, 1281
 Liu, C., Bailer-Jones, C. A. L., Sordo, R., et al. 2012, *ArXiv e-prints* (1207.6005)
 Martić, M., Lebrun, J.-C., Appourchaux, T., & Korzennik, S. G. 2004, *A&A*, 418, 295
 Morel, T. & Miglio, A. 2012, *MNRAS*, 419, L34
 Mosser, B., Elsworth, Y., Hekker, S., et al. 2012, *A&A*, 537, A30
 North, J. R., Davis, J., Bedding, T. R., et al. 2007, *MNRAS*, 380, L80
 Porto de Mello, G. F., Lyra, W., & Keller, G. R. 2008, *A&A*, 488, 653
 Pourbaix, D., Nidever, D., McCarthy, C., et al. 2002, *A&A*, 386, 280
 Toutain, T. & Froehlich, C. 1992, *A&A*, 257, 287
 Verner, G. A., Elsworth, Y., Chaplin, W. J., et al. 2011, *MNRAS*, 415, 3539